Reduced poleward transport due to stratospheric heating under geoengineering

Daniele Visioni [1], Douglas G. MacMartin [1], Ben Kravitz [2,3], Walker Lee [1], Isla R. Simpson [4], Jadwiga H. Richter [4]

[1]Sibley School for Mechanical and Aerospace Engineering, Cornell University, Ithaca, NY
[2]Department of Earth and Atmospheric Science, Indiana University, Bloomington, IN
[3]Atmospheric Sciences and Global Change Division, Pacific Northwest National Laboratory, Richland, WA, USA
[4]Climate and Global Dynamics Laboratory, National Center for Atmospheric Research, Boulder, CO, USA

Key Points:

- The stratospheric injection of SO_2 would result in localized stratospheric warming
- This warming would modify the thermal wind balance, strengthening the stratospheric polar vortexes
- This results in less poleward transport of the aerosols, requiring more SO2 to achieve the desired cooling

Corresponding author: Daniele Visioni, daniele.visioni@cornell.edu

Abstract

By injecting SO_2 into the stratosphere at different latitudes, it might be possible to not only reduce global mean surface temperature compared to the warming produced by greenhouse gases, but also to minimize changes in the equator-to-pole and inter-hemispheric gradients of surface temperature, further reducing some of the impacts arising from climate change relative to equatorial SO_2 injection. This can happen only if the resulting sulfate aerosols are transported to higher latitudes by the stratospheric circulation, ensuring that a greater part of the solar radiation is reflected back to space at higher latitudes, compensating for the reduced sunlight there. However, the stratospheric heating produced by these aerosols modifies the global circulation and strengthens the stratospheric polar vortex that acts as a barrier to the transport of air towards the poles. We show how this stratospheric heating results in a nonlinear feedback where increasing injection rates lead to a stronger high latitudinal transport barrier. This implies a potential limitation in the high-latitude aerosol burden and subsequent high-latitude cooling.

Plain Language Summary

If we were to inject aerosols at high altitudes in order to reflect some incoming solar radiation and cool the planet, it would result in a localized warming at those altitudes. This would affect the circulation of air masses, and we show here that it would strengthen the intensity of the polar vortexes that control the transport of air from the mid-latitudes to the poles. If this transport is inhibited, less aerosol can reach the high latitudes, and obtaining the correct distribution of aerosols needed to achieve the required climate goals to avoid unintended impacts is made harder.

1 Introduction

Stratospheric aerosol geoengineering (SAG) involves deliberately injecting aerosols or their precursors into the stratosphere in an attempt to cool the planet, mimicking the cooling seen after large volcanic eruptions (Budyko, 1978; Crutzen, 2006). Climate model simulations generally agree that injecting SO_2 has the potential to reduce global surface temperatures relative to the warming induced by greenhouse gases (GHGs); the imperfect compensation between the GHG and SO_2 forcing (Govindasamy et al., 2003; Jiang et al., 2019) would, however, result in differences in aspects of the surface climate such as the hydrological cycle (Tilmes et al., 2013; Niemeier et al., 2013; I. Simpson et al., 2019) compared to a non-geoengineered climate with no GHG warming, but these differences would still be much lower than those resulting from continued GHG induced warming (Irvine & Keith, 2020). Large uncertainties are still present in many areas related to the possible interactions with different aspects of the climate (Kravitz & MacMartin, 2020).

One of the most important perturbations resulting from the injection of SO_2 is the stratospheric heating resulting from the increase in aerosol heating rates. Modifications in the stratospheric transport, observed in the past in the case of large volcanic eruptions (Robock, 2000; Pitari et al., 2016), are consistently found in simulations (Niemeier & Schmidt, 2017; Richter et al., 2017; Visioni et al., 2017; Kleinschmitt et al., 2018). Aquila et al. (2014) first pointed out the potential of equatorial SAG to interact with stratospheric dynamics by modifying the quasi-biennial oscillation (QBO), resulting, for high enough loads of injection, in a permanent locking of the QBO in a Westerly-phase. That phase of the QBO results in stronger aerosol confinement in the tropical pipe due to decreased meridional transport and increased residual vertical velocities, which result in greater sulfate aerosol growth (Niemeier & Schmidt, 2017; Visioni et al., 2018; Kravitz et al., 2019). Larger sulfate aerosols are less effective at backscattering insolation and have reduced particle lifetimes (Pierce et al., 2010), reducing the SO_4 burden and resulting global aerosol optical depth (AOD) that results from a given SO_2 injection rate. Some studies (Pierce et al., 2010; Benduhn et al., 2016) have proposed that the injection of

H_2SO_4 droplets instead of SO_2 might produce an aerosol size distribution with smaller particles, capable of reflecting more solar radiation per unit mass (Dykema et al., 2016), thus potentially reducing some of the side effects related to the heating produced by the aerosols (Vattioni et al., 2019); other aerosol choices might result in less, or even no, stratospheric heating (Keith et al., 2016).

Injecting outside of the equator has been shown to better manage desired temperature targets, and to reduce some of the side-effects of equatorial injections mentioned above (Tilmes et al., 2017; Tilmes, Richter, Mills, et al., 2018; Richter et al., 2017; Dai et al., 2018; Kravitz et al., 2019). By injecting at 15°N, 30°N, 15°S and 30°S in the Geoengineering Large Ensemble simulations performed with the Community Earth System Model (CESM1(WACCM)), it was possible to produce a stratospheric aerosol layer capable of reducing global mean temperatures over the course of the 21st century as well as restoring the inter-hemispheric and equator-to-pole temperature gradients affected by the increasing GHGs concentration. Managing these additional temperature goals, however, requires part of the aerosol distribution to reach the very high latitudes.

A strong stratospheric polar vortex inhibits aerosol transport to high latitudes and results in greater confinement of polar stratospheric air. As such, one measure of the transport of stratospheric air from the mid latitudes to the poles is the strength of the stratospheric polar vortex (Waugh et al., 2017). In the two hemispheres, westerly zonal winds at and above 50 hPa have a peak in strength at approximately 60° latitude in winter. Projecting future changes in the polar vortex is difficult, as they will be influenced by stratospheric cooling from GHGs, as well as projected reductions in ozone-depleting substances (ODS, Dhomse et al., 2018). Models tend to disagree on the sign and magnitude of net vortex changes (Butchart et al., 2010; Manzini et al., 2014; I. R. Simpson et al., 2018; Wu et al., 2019).

In this work we show that, for SAG simulations, the perturbation produced by the stratospheric heating even in non-equatorial SAG results in a strengthening of the polar vortex in both hemispheres, resulting in a reduced transport of aerosols from the mid latitudes to the poles, and, ultimately, in decreased high-latitude AOD per Tg-SO_2 injected. This points to a fundamental limit in the controllability of the aerosol cloud without additional injection poleward of the polar vortex.

2 Methods

The simulations analyzed in this paper have been performed with the Community Earth System Model (CESM1(WACCM)), with a resolution of 0.95° × 1.25°, 70 vertical levels and fully interactive stratospheric chemistry (Mills et al., 2017). CESM1(WACCM) capabilities in representing stratospheric dynamics have been discussed in depth in the available literature for historical simulations (Dietmuller et al., 2018), and the model validates well against previous large tropical volcanic eruptions (Mills et al., 2016, 2017).

The analyses presented here are based on two ensembles of SAG simulations. The first, the Geoengineering Large Ensemble (GLENS; Tilmes, Richter, Kravitz, et al., 2018), involves independently modifying the annual SO_2 injection (5 km above the mean tropopause) rate at 30°N, 15°N, 15°S, and 30°S to maintain (against a background of RCP8.5) three independent temperature metrics at their 2010-2030 average levels: global mean temperature, the inter-hemispheric temperature gradient, and the equator-to-pole temperature gradient. The second ensemble, labeled GEQ, involves modifying the annual SO_2 injection rate at the equator to maintain global mean temperature at its 2010-2030 average level, also against a background of RCP8.5 (Kravitz et al., 2019). These objectives were met using a feedback algorithm (Kravitz et al., 2016, 2017) to independently adjust the SO_2 injection rates at each location based on past departures from the intended temperature targets. An ensemble of 21 baseline simulations were conducted with RCP8.5 from 2010 to 2030; four of these were extended until at least 2098. The 21-member GLENS ensemble branched from these simulations in 2020 and were run until 2100. In GLENS

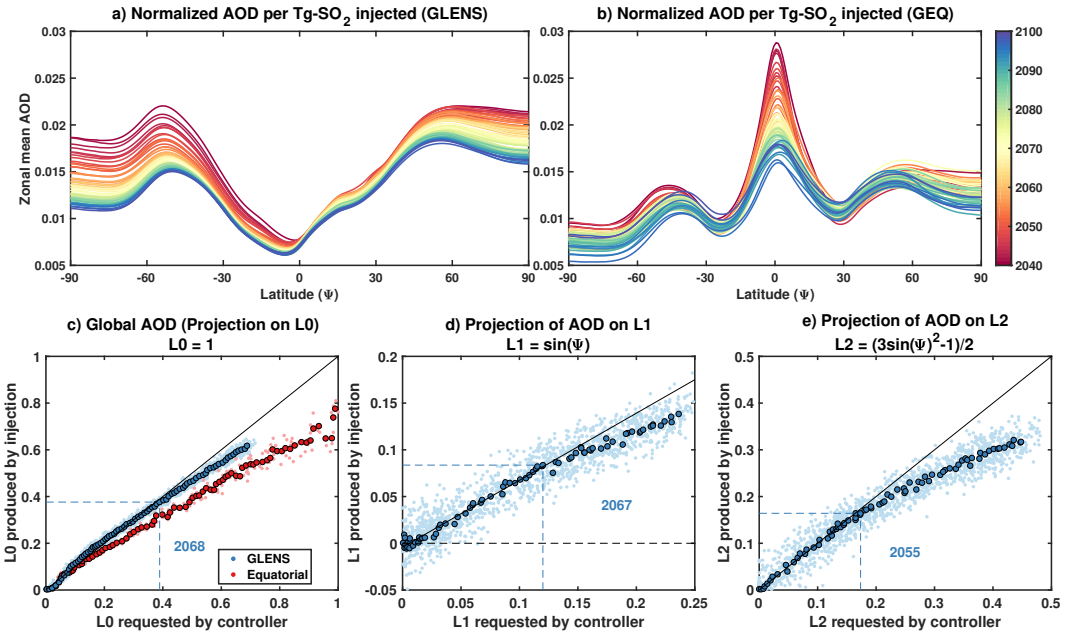

Figure 1. Top panels: Zonal mean AOD (a) for GLENS, and (b) for GEQ normalized to the amount of SO_2 injected in the year before, and color-coded by year. Bottom panels: projections of AOD onto the first three Legendre polynomials; the ability to choose injection rates at different latitudes to independently alter these patterns of AOD is used by the controller to manage global mean temperature (using global mean AOD, L0, shown in panel c), inter-hemispheric temperature gradient (using AOD projected over a linearly increasing function from south to north, L1, shown in panel d) and equator-to-pole temperature gradient (using AOD projected over a quadratic function maximized at the poles and minimized at the equator, L2, shown in panel e). The values requested by the controller in each year are plotted against the actual L0, L1, and L2 values of the AOD. A linear fit for small values of the three quantities is provided, with the threshold where the linear relationship stops being true highlighted.

and RCP8.5, the baseline simulations were conducted from 2010 to 2030 under RCP8.5 forcing for 21 ensemble members, and four of these ensemble members were extended up to at least 2098. For GEQ, 3 simulations were conducted.

3 Results

In GLENS, annual mean global average AOD and tropical stratosphere sulfate aerosol effective radius both scale proportionally with the annual SO_2 injection rate (Tilmes, Richter, Kravitz, et al., 2018). This result differs from earlier results given for equatorial injections (Niemeier & Timmreck, 2015) and has been concluded to be a direct result of the injection strategy (Tilmes, Richter, Kravitz, et al., 2018; Kravitz et al., 2019). In Fig. 1 we show that this conclusion mostly holds true when looking at globally averaged AOD because the globally averaged value heavily weights tropical latitudes, where the linear scaling holds. In the extra-tropics, the relationship between AOD and injection rate is, on the other hand, non-constant. To highlight the difference between the two injection strategies, Fig. 1b shows the same values for GEQ, where there is a clear sublinear relationship between SO_2 injection rate and AOD in the tropical pipe, which we attribute to the microphysical effects discussed previously.

The effects of this "diminishing return" in the efficiency of the injection at high latitudes is shown in the bottom panels in Fig. 1, depicting zonally averaged AOD projected onto the first three Legendre polynomials (termed L0, L1, and L2). As shown in previous works (Ban-Weiss & Caldeira, 2010; Kravitz et al., 2016) the solar constant can be reduced across these three idealized patterns to not only reduce global mean temperature (termed T0) but also to maintain the inter-hemispheric temperature gradient (T1) and equator-to-pole temperature gradient (T2). By means of injecting at different latitudes it has been shown that it is possible to achieve similar spatial patterns for AOD, capable of reflecting sunlight across the three patterns and thus achieving the three temperature goals (MacMartin et al., 2017). The correlation between injected SO_2 at the four locations and resulting SO_2 in MacMartin et al. (2017), assuming that the relationship would remain linear for different injection loads.

From the bottom panels in Fig. 1, it is clear that the assumptions of linearity in the response of L0 and L1 holds robustly up to approximately 2070, or roughly 30 Tg-SO_2 injected overall, but linearity subsequently breaks down, leading to a decrease in efficiency (by which here we mean the ratio of produced AOD to injected aerosol precursors is lower) at high latitudes.

Unlike for the equatorial case, this high-latitude effect is not due to microphysical changes in the radius of the sulfate particles, since we show in Fig. S1 that the radii change less at high latitudes compared to tropical latitudes (20% compared to 50% over the course of 60 years of increasing injection rates), compared to the changes in AOD shown in Fig. 1. We identify this effect as being due to an overall strengthening of the stratospheric polar vortex due to changes in the thermal wind balance, caused by the strong temperature gradient in the tropical stratosphere produced by the aerosols. In Fig. 2 we show the strength of the mean zonal wind (U) in the winter months at 50 hPa and 60° latitude both in the NH and SH. Changes in the overall structure of the zonal winds have been noted before (Niemeier & Schmidt, 2017; Richter et al., 2017; Kravitz et al., 2019; Niemeier et al., 2020), but their temporal variations have not been analyzed.

To better identify changes in the transport barrier associated with the polar vortex we use here Ertel's Potential Vorticity (PV) as a diagnostic tool. This quantity has already been used in the past to further verify changes in the transport of various chemical components in the atmosphere due to circulation changes, especially at high latitudes. (Manney et al., 1994; Nash et al., 1996; Ploeger et al., 2015). In the absence of friction and diabatic processes, the PV of an air parcel is materially conserved. Thus, it should be expected that in regions of enhanced PV gradient, there is reduced exchange of air parcels and, therefore, reduced mixing of atmospheric constituents across that gradient (Holton, 2004). Manney et al. (1994); Nash et al. (1996) proved that this analogy is successful in identifying transport barriers due to strengthening of the stratospheric polar vortex, resulting in reduced mixing of warm air from lower latitudes and, therefore, a cooler polar stratosphere with subsequent ozone destruction. We show in Fig. 3 the stratospheric PV gradient in the 2010-2029 period, from which are clearly visible the transport barriers both in the tropics (when considering the annual mean) and at high latitudes (in the relative hemispheric winter). While the effect of the polar barriers is visible in both injection strategies when considering the AOD in Fig. 1, the effect of the tropical barrier is also visible in the equatorial injection strategy, that presents clear minima in proximity of the tropical transport barrier (that are also strengthened due to the locking of the QBO in the W phase in this case (Kravitz et al., 2019)).

In Fig. 4 we show that the PV gradient in both hemispheres in winter has a strong positive anomaly that evolves with increasing injection rates. There appear to be differences in the response between the hemispheres: namely, that the transport barrier appears to slightly shift in the northern hemisphere (both pole-ward and equator-ward depending on the decade), but to more consistently shift equator-ward in the southern one. While the magnitude of the maxima in both gradient anomalies increases in both hemispheres in a similar way, the differences in the latitudinal shift could be due to a slight asymmetry in the temperature anomaly in the tropics, due to differences in the injec-

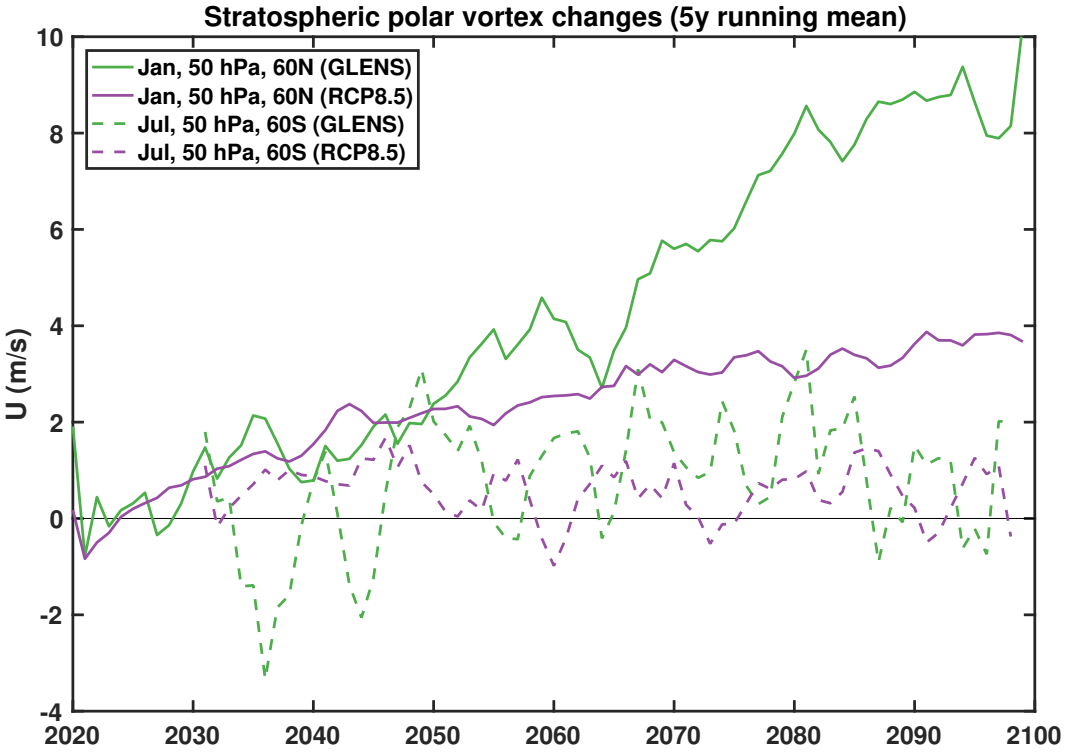

Figure 2. Changes in U winds at 50 hPa at 60° in both hemispheres in the month where the strength of the polar vortex is highest, for both GLENS (straight line) and RCP8.5 (dashed line), compared against the RCP8.5 period between 2010 and 2029.

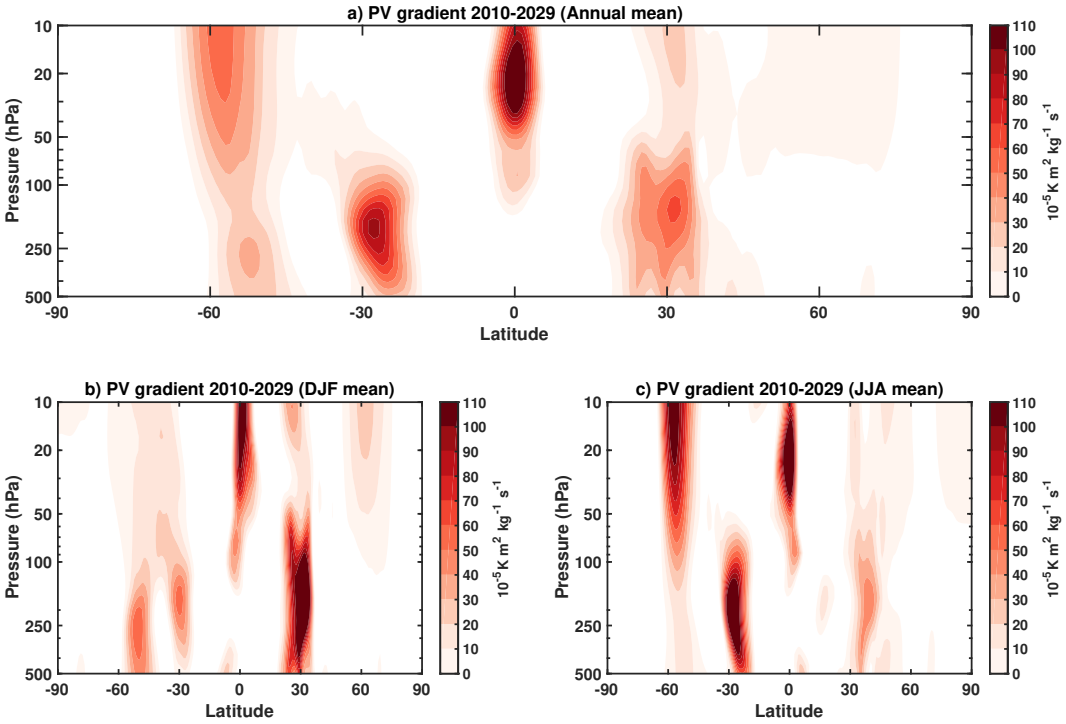

Figure 3. PV gradient averaged over the 2010-2029 period in RCP8.5, considering the annual average (panel a) and the average over the related hemispheric winter months (panels b and c).

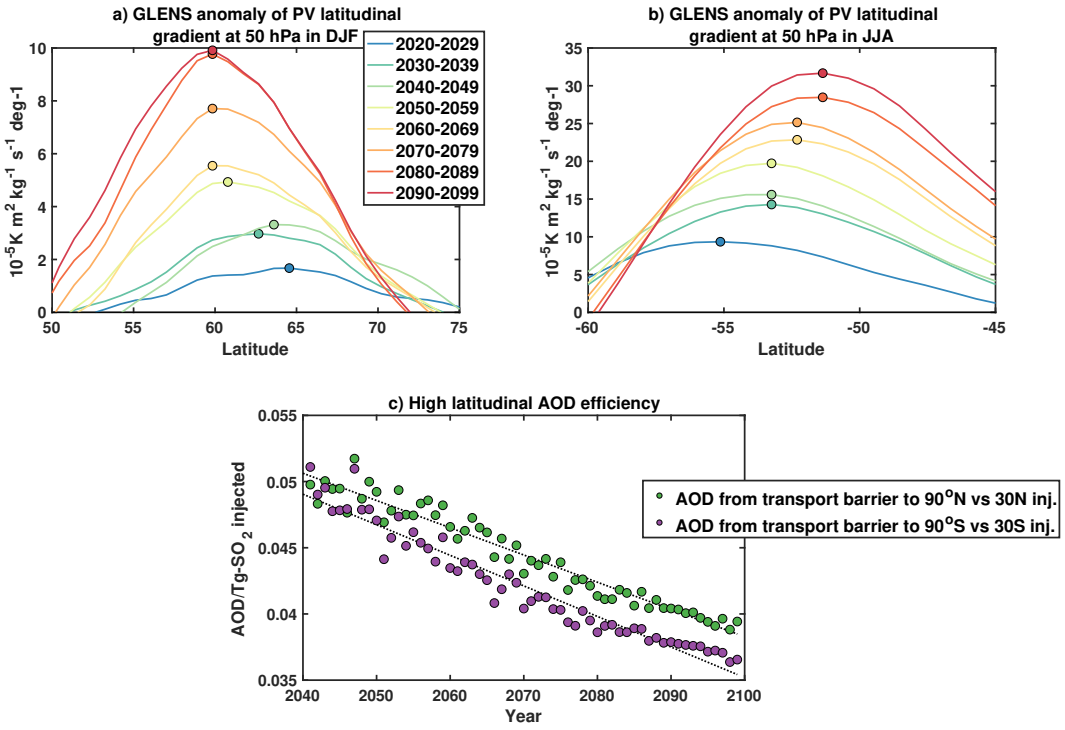

Figure 4. Changes in the PV gradient anomaly compared to the 2010-2029 period at 50 hPa in the month where the strength of the polar vortex is higher (a), DJF, Northern Hemisphere; b), JJA, Southern Hemisphere), divided by decade (see legend). The average location of the maxima is highlighted in each decade with a circle of the same color. Panel c) Yearly AOD averaged from 90° to the transport barrier identified using the PV gradient anomalies, normalized by the injection rate in that year at 30°. A graphical linear fit is provided for both quantities.

tion rates in the hemispheres. In Fig. S3 and Fig. S4 we further show for each decade the zonal mean PV anomaly at different latitudes and altitudes, highlighting the relationship between PV anomaly and changes in the zonal winds identified in Fig. 3. The dynamics and structure of the polar vortex in each hemisphere are different, and also in our case there could be a variety of reasons why they might not respond exactly the same way. We note that the stratospheric polar vortex is generally already stronger in the southern hemisphere (see Fig. S2), and while this is observed also in reanalyses, CESM1(WACCM) has an already identified strong bias in the southern polar vortex (Mills et al., 2017).

One possible further explanation for both the changes in location and overall interhemispheric differences in the evolution over time could be found in differences in the ozone response: by 2050, ODS concentrations are projected to reduce following a strong abatement in emissions, resulting in a full recovery of stratospheric ozone (and possible super-recovery, due to stratospheric cooling from GHGs) late in the 21st century (Dhomse et al., 2018). The heating produced by the sulfate aerosols can contribute to ozone destruction (Tilmes, Richter, Kravitz, et al., 2018; Richter et al., 2017) by Cl_y and Br_y, therefore resulting in a net cooling attributable to ozone at high latitudes. When the concentration of ODS is reduced, however, this mechanism of ozone destruction weakens, and ozone is allowed to recover also in the geoengineering case (albeit less than under RCP8.5). This then produces a positive change in the heating rates produced by ozone, particularly in the SH where ozone destruction was stronger in the 2010-2029 period (Fig. S6). The high-latitude positive heating rates after 2050 may partially counter-balance the tem-

perature gradient resulting from the aerosol heating rates at lower latitudes, therefore modifying the changes in the SH stratospheric polar vortex.

Finally, in Fig. 4c we use the transport barrier identified in the previous discussion to consider the AOD at high latitudes as only that which resides poleward of the latitude of the maximum of the PV anomaly gradient. Normalizing this AOD to the injection rate at 30° in both hemispheres, we show how this "high latitudinal efficiency" decreases over time given the strengthening of the polar vortexes. We only show the values starting in 2040 (as in Fig. 1) for two main reasons: one is that before that date, the algorithm that determines the injection rates has not yet converged, resulting in higher year to year differences in the injection rates and in differences in the demand for L1 and L2 ((see also Tilmes, Richter, Kravitz, et al., 2018). The second is that, as shown in Fig. 4 and Fig. S3 and S4, changes in the stratospheric vortex are less clear prior to 2040. The behavior is very similar between the two hemispheres, with slightly lower values for the AOD in the southern hemisphere that can be explained by the general greater strength of the polar vortex discussed above.

4 Conclusions

If sulfate geoengineering is to be investigated as a potential measure to partially counteract the surface warming resulting from the increase in GHGs over this century, particular attention should be devoted to both its potential surface effects (I. Simpson et al., 2019; Irvine & Keith, 2020) and to understanding its fundamental limitations. Previous work has shown that the effectiveness when injecting sulfate only at the equator is somehow limited for very high injection loads due to microphysical constraints (Niemeier & Timmreck, 2015), modifications of equatorial dynamics (Aquila et al., 2014) and the interplay between these two (Visioni et al., 2018). Injecting outside the equator has been shown to have the potential to reduce some side effects (Kravitz et al., 2019) and to offer further controllability in terms of achievable climate goals through further control of the resulting latitudinal optical depth of the aerosols (MacMartin et al., 2017; Kravitz et al., 2017; Tilmes, Richter, Kravitz, et al., 2018). Even this approach, however, does not completely reduce the warming at high latitudes: this is partially due to an imperfect match between the radiative forcing of the aerosols (dependent on the presence of incoming solar radiation) compared to that of the CO_2 (Govindasamy et al., 2003; Jiang et al., 2019).

Here we show that another factor to consider when discussing potential limitations of SAG is the modification of stratospheric circulation induced by the stratospheric heating, especially that produced by aerosols at high latitudes: changes to the thermal wind balance result, in our model simulations, in a strengthening of the stratospheric polar vortex, with subsequent increased isolation of polar air resulting in a reduction in the amount of sulfate aerosols that can be moved by the Brewer-Dobson circulation from medium to high latitudes. While this only slightly affects the ability to reduce global mean surface temperatures, it does influence the desired distribution of AOD at high latitude, resulting in an increased difficulty in maintaining the equator-to-pole temperature gradient that needs to be corrected (and is, in our simulations, mostly corrected by the implemented feedback algorithm) by increasing the injection amount more than it would be if this effect was not present (thus possibly increasing side effects related to sulfate deposition, (Visioni et al., 2020)). Ozone changes driven mostly by a reduction of ozone depleting substances at high latitudes, but also partially by the aerosols, might also play a role.

In conclusion, this points to the existence of a fundamental limit in the ability of SAG to reduce surface temperature at high latitudes: if the amount of cooling desired is too high, the stratospheric interactions of the aerosols themselves partially reduce the ability of the aerosols to cool.

Acknowledgments

We would like to acknowledge high-performance computing support from Cheyenne (doi:10.5065/D6RX99HX) provided by NCAR's Computational and Information Systems Laboratory, sponsored by the National Science Foundation. Support for D. V. and D. G. M. was provided by the Atkinson Center for a Sustainable Future at Cornell University and by the National Science Foundation through agreement CBET-1818759. Support for B.K. was provided in part by the National Science Foundation through agreement CBET-1931641, the Indiana University Environmental Resilience Institute, and the Prepared for Environmental Change Grand Challenge initiative. The Pacific Northwest National Laboratory is operated for the US Department of Energy by Battelle Memorial Institute under contract DE-AC05-76RL01830. All data used in this article is available at https://doi.org/10.5065/D6JH3JXX.

References

Aquila, V., Garfinkel, C., Newman, P., Oman, L., & Waugh, D. (2014). Modifications of the quasi-biennial oscillation by a geoengineering perturbation of the stratospheric aerosol layer. *Geophysical Research Letters*, *41*(5), 1738–1744.

Ban-Weiss, G. A., & Caldeira, K. (2010). Geoengineering as an optimization problem. *Environmental Research Letters*, *5*(3). doi: 10.1088/1748-9326/5/3/034009

Benduhn, F., Schallock, J., & Lawrence, M. G. (2016). Early growth dynamical implications for the steerability of stratospheric solar radiation management via sulfur aerosol particles. *Geophysical Research Letters*, *43*(18), 9956-9963. Retrieved from `https://agupubs.onlinelibrary.wiley.com/doi/abs/10.1002/2016GL070701` doi: 10.1002/2016GL070701

Budyko, M. I. (1978). *The climate of the future*. American Geophysical Union. Retrieved from `http://dx.doi.org/10.1002/9781118665251.ch7` doi: 10.1002/9781118665251.ch7

Butchart, N., Cionni, I., Eyring, V., Shepherd, T. G., Waugh, D. W., Akiyoshi, H., ... Tian, W. (2010). Chemistry–climate model simulations of twenty-first century stratospheric climate and circulation changes. *Journal of Climate*, *23*(20), 5349-5374. Retrieved from `https://doi.org/10.1175/2010JCLI3404.1` doi: 10.1175/2010JCLI3404.1

Crutzen, P. J. (2006). Albedo enhancement by stratospheric sulfur injections: A contribution to resolve a policy dilemma? *Climatic Change*, *77*(3), 211–220. Retrieved from `http://dx.doi.org/10.1007/s10584-006-9101-y` doi: 10.1007/s10584-006-9101-y

Dai, Z., Weisenstein, D. K., & Keith, D. W. (2018). Tailoring Meridional and Seasonal Radiative Forcing by Sulfate Aerosol Solar Geoengineering. *Geophysical Research Letters*, *45*(2), 1030–1039. doi: 10.1002/2017GL076472

Dhomse, S. S., Kinnison, D., Chipperfield, M. P., Salawitch, R. J., Cionni, I., Hegglin, M. I., ... Zeng, G. (2018). Estimates of ozone return dates from Chemistry-Climate Model Initiative simulations. *Atmospheric Chemistry and Physics*, *18*(11), 8409–8438. doi: 10.5194/acp-18-8409-2018

Dietmuller, S., Eichinger, R., Garny, H., Birner, T., Boenisch, H., Pitari, G., ... Schofield, R. (2018). Quantifying the effect of mixing on the mean age of air in ccmval-2 and ccmi-1 models. *Atmospheric Chemistry and Physics*, *18*(9), 6699–6720. Retrieved from `https://www.atmos-chem-phys.net/18/6699/2018/` doi: 10.5194/acp-18-6699-2018

Dykema, J. A., Keith, D. W., & Keutsch, F. N. (2016). Improved aerosol radiative properties as a foundation for solar geoengineering risk assessment. *Geophysical Research Letters*, *43*(14), 7758-7766. Retrieved from `https://agupubs.onlinelibrary.wiley.com/doi/abs/10.1002/2016GL069258` doi: 10.1002/2016GL069258

Govindasamy, B., Caldeira, K., & Duffy, P. (2003). Geoengineering earth's

radiation balance to mitigate climate change from a quadrupling of co2. *Global and Planetary Change*, *37*(1), 157 - 168. Retrieved from http://www.sciencedirect.com/science/article/pii/S0921818102001959 (Evaluation, Intercomparison and Application of Global Climate Models) doi: https://doi.org/10.1016/S0921-8181(02)00195-9

Holton, J. R. (2004). Chapter 4 circulation and vorticity. In J. R. Holton (Ed.), *An introduction to dynamic meteorology* (Vol. 88, p. 86 - 114). Academic Press. Retrieved from http://www.sciencedirect.com/science/article/pii/S007461420480038X doi: https://doi.org/10.1016/S0074-6142(04)80038-X

Irvine, P. J., & Keith, D. W. (2020, mar). Halving warming with stratospheric aerosol geoengineering moderates policy-relevant climate hazards. *Environmental Research Letters*, *15*(4), 044011. doi: 10.1088/1748-9326/ab76de

Jiang, J., Cao, L., MacMartin, D. G., Simpson, I. R., Kravitz, B., Cheng, W., ... Mills, M. J. (2019). Stratospheric Sulfate Aerosol Geoengineering Could Alter the High-Latitude Seasonal Cycle. *Geophysical Research Letters*, *46*(23), 14153–14163. doi: 10.1029/2019GL085758

Keith, D. W., Weisenstein, D. K., Dykema, J. A., & Keutsch, F. N. (2016). Stratospheric solar geoengineering without ozone loss. *Proceedings of the National Academy of Sciences*, *113*(52), 14910–14914. Retrieved from https://www.pnas.org/content/113/52/14910 doi: 10.1073/pnas.1615572113

Kleinschmitt, C., Boucher, O., & Platt, U. (2018). Sensitivity of the radiative forcing by stratospheric sulfur geoengineering to the amount and strategy of the so2 injection studied with the lmdz-s3a model. *Atmospheric Chemistry and Physics*, *18*(4), 2769–2786. Retrieved from https://www.atmos-chem-phys.net/18/2769/2018/ doi: 10.5194/acp-18-2769-2018

Kravitz, B., Lamarque, J.-F., Tribbia, J. J., Tilmes, S., Vitt, F., Richter, J. H., ... Mills, M. J. (2017). First Simulations of Designing Stratospheric Sulfate Aerosol Geoengineering to Meet Multiple Simultaneous Climate Objectives. *Journal of Geophysical Research: Atmospheres*, *122*(23), 12,616–12,634. doi: 10.1002/2017jd026874

Kravitz, B., & MacMartin, D. G. (2020). Uncertainty and the basis for confidence in solar geoengineering research. *Nature Reviews Earth & Environment*, *1*(1), 64–75. Retrieved from http://dx.doi.org/10.1038/s43017-019-0004-7{\%}0Ahttp://www.nature.com/articles/s43017-019-0004-7 doi: 10.1038/s43017-019-0004-7

Kravitz, B., MacMartin, D. G., Tilmes, S., Richter, J. H., Mills, M. J., Cheng, W., ... Vitt, F. (2019). Comparing surface and stratospheric impacts of geoengineering with different so2 injection strategies. *Journal of Geophysical Research: Atmospheres*, *124*(14), 7900-7918. Retrieved from https://agupubs.onlinelibrary.wiley.com/doi/abs/10.1029/2019JD030329 doi: 10.1029/2019JD030329

Kravitz, B., MacMartin, D. G., Wang, H., & Rasch, P. J. (2016). Geoengineering as a design problem. *Earth System Dynamics*, *7*(2), 469–497. doi: 10.5194/esd-7-469-2016

MacMartin, D. G., Kravitz, B., Mills, M. J., Tribbia, J. J., Tilmes, S., Richter, J. H., ... Lamarque, J.-F. (2017). The Climate Response to Stratospheric Aerosol Geoengineering Can Be Tailored Using Multiple Injection Locations. *Journal of Geophysical Research: Atmospheres*, *122*(23), 12,574–12,590. doi: 10.1002/2017jd026868

Manney, G. L., Zurek, R. W., Gelman, M. E., Miller, A. J., & Nagatani, R. (1994). The anomalous arctic lower stratospheric polar vortex of 1992–1993. *Geophysical Research Letters*, *21*(22), 2405-2408. Retrieved from https://agupubs.onlinelibrary.wiley.com/doi/abs/10.1029/94GL02368 doi: 10.1029/94GL02368

Manzini, E., Karpechko, A. Y., Anstey, J., Baldwin, M. P., Black, R. X., Cagnazzo,

C., ... Zappa, G. (2014). Northern winter climate change: Assessment of uncertainty in cmip5 projections related to stratosphere-troposphere coupling. *Journal of Geophysical Research: Atmospheres*, *119*(13), 7979-7998. Retrieved from https://agupubs.onlinelibrary.wiley.com/doi/abs/10.1002/2013JD021403 doi: 10.1002/2013JD021403

Mills, M. J., Richter, J. H., Tilmes, S., Kravitz, B., Macmartin, D. G., Glanville, A. A., ... Kinnison, D. E. (2017). Radiative and chemical response to interactive stratospheric sulfate aerosols in fully coupled CESM1(WACCM). *Journal of Geophysical Research: Atmospheres*, *122*(23), 13,061–13,078. doi: 10.1002/2017JD027006

Mills, M. J., Schmidt, A., Easter, R., Solomon, S., Kinnison, D. E., Ghan, S. J., ... Gettelman, A. (2016). Global volcanic aerosol properties derived from emissions, 1990–2014, using cesm1(waccm). *Journal of Geophysical Research: Atmospheres*, *121*(5), 2332-2348. Retrieved from https://agupubs.onlinelibrary.wiley.com/doi/abs/10.1002/2015JD024290 doi: 10.1002/2015JD024290

Nash, E. R., Newman, P. A., Rosenfield, J. E., & Schoeberl, M. R. (1996). An objective determination of the polar vortex using ertel's potential vorticity. *Journal of Geophysical Research: Atmospheres*, *101*(D5), 9471-9478. Retrieved from https://agupubs.onlinelibrary.wiley.com/doi/abs/10.1029/96JD00066 doi: 10.1029/96JD00066

Niemeier, U., Richter, J. H., & Tilmes, S. (2020). Differing responses of the qbo to so2 injections in two global models. *Atmospheric Chemistry and Physics Discussions*, *2020*, 1–21. Retrieved from https://www.atmos-chem-phys-discuss.net/acp-2020-206/ doi: 10.5194/acp-2020-206

Niemeier, U., & Schmidt, H. (2017). Changing transport processes in the stratosphere by radiative heating of sulfate aerosols. *Atmospheric Chemistry and Physics*, *17*(24), 14871–14886. Retrieved from https://www.atmos-chem-phys.net/17/14871/2017/ doi: 10.5194/acp-17-14871-2017

Niemeier, U., Schmidt, H., Alterskjær, K., & Kristjánsson, J. E. (2013). Solar irradiance reduction via climate engineering: Impact of different techniques on the energy balance and the hydrological cycle. *Journal of Geophysical Research: Atmospheres*, *118*(21), 11,905-11,917. Retrieved from https://agupubs.onlinelibrary.wiley.com/doi/abs/10.1002/2013JD020445 doi: 10.1002/2013JD020445

Niemeier, U., & Timmreck, C. (2015). What is the limit of climate engineering by stratospheric injection of so_2? *Atmospheric Chemistry and Physics*, *15*(16), 9129–9141. Retrieved from https://www.atmos-chem-phys.net/15/9129/2015/ doi: 10.5194/acp-15-9129-2015

Pierce, J. R., Weisenstein, D. K., Heckendorn, P., Peter, T., & Keith, D. W. (2010). Efficient formation of stratospheric aerosol for climate engineering by emission of condensible vapor from aircraft. *Geophysical Research Letters*, *37*(18). Retrieved from https://agupubs.onlinelibrary.wiley.com/doi/abs/10.1029/2010GL043975 doi: 10.1029/2010GL043975

Pitari, G., Genova, G. D., Mancini, E., Visioni, D., Gandolfi, I., & Cionni, I. (2016). Stratospheric aerosols from major volcanic eruptions: A composition-climate model study of the aerosol cloud dispersal and e-folding time. *Atmosphere*. Retrieved from http://www.scopus.com/inward/record.url?eid=2-s2.0-84976884421{\&}partnerID=MN8TOARS doi: 10.3390/atmos7060075

Ploeger, F., Gottschling, C., Griessbach, S., Grooß, J.-U., Guenther, G., Konopka, P., ... von Hobe, M. (2015). A potential vorticity-based determination of the transport barrier in the asian summer monsoon anticyclone. *Atmospheric Chemistry and Physics*, *15*(22), 13145–13159. Retrieved from https://www.atmos-chem-phys.net/15/13145/2015/ doi: 10.5194/acp-15-13145-2015

Richter, J. H., Tilmes, S., Mills, M. J., Tribbia, J. J., Kravitz, B., Macmartin, D. G., ... Lamarque, J. F. (2017). Stratospheric dynamical response and ozone feedbacks in the presence of so2 injections. *Journal of Geophysical Research: Atmospheres*, *122*(23), 12,557–12,573. doi: 10.1002/2017JD026912

Robock, A. (2000). Volcanic eruptions and climate. *Reviews of Geophysics*, *38*(2), 191-219. Retrieved from https://agupubs.onlinelibrary.wiley.com/doi/abs/10.1029/1998RG000054 doi: 10.1029/1998RG000054

Simpson, I., Tilmes, S., Richter, J., Kravitz, B., MacMartin, D., Mills, M., ... Pendergrass, A. (2019). The regional hydroclimate response to stratospheric sulfate geoengineering and the role of stratospheric heating. *Journal of Geophysical Research: Atmospheres*, 2019JD031093. Retrieved from https://onlinelibrary.wiley.com/doi/abs/10.1029/2019JD031093 doi: 10.1029/2019JD031093

Simpson, I. R., Hitchcock, P., Seager, R., Wu, Y., & Callaghan, P. (2018). The downward influence of uncertainty in the northern hemisphere stratospheric polar vortex response to climate change. *Journal of Climate*, *31*(16), 6371-6391. Retrieved from https://doi.org/10.1175/JCLI-D-18-0041.1 doi: 10.1175/JCLI-D-18-0041.1

Tilmes, S., Fasullo, J., Lamarque, J.-F., Marsh, D. R., Mills, M., Alterskjær, K., ... Watanabe, S. (2013). The hydrological impact of geoengineering in the geoengineering model intercomparison project (geomip). *Journal of Geophysical Research: Atmospheres*, *118*(19), 11,036-11,058. Retrieved from https://agupubs.onlinelibrary.wiley.com/doi/abs/10.1002/jgrd.50868 doi: 10.1002/jgrd.50868

Tilmes, S., Richter, J. H., Kravitz, B., Macmartin, D. G., Mills, M. J., Simpson, I. R., ... Ghosh, S. (2018). CESM1(WACCM) stratospheric aerosol geoengineering large ensemble project. *Bulletin of the American Meteorological Society*, *99*(11), 2361–2371. doi: 10.1175/BAMS-D-17-0267.1

Tilmes, S., Richter, J. H., Mills, M. J., Kravitz, B., MacMartin, D. G., Garcia, R. R., ... Vitt, F. (2018). Effects of Different Stratospheric SO2 Injection Altitudes on Stratospheric Chemistry and Dynamics. *Journal of Geophysical Research: Atmospheres*, *123*(9), 4654–4673. doi: 10.1002/2017JD028146

Tilmes, S., Richter, J. H., Mills, M. J., Kravitz, B., Macmartin, D. G., Vitt, F., ... Lamarque, J. F. (2017). Sensitivity of aerosol distribution and climate response to stratospheric SO2 injection locations. *Journal of Geophysical Research: Atmospheres*, *122*(23), 12,591–12,615. doi: 10.1002/2017JD026888

Vattioni, S., Weisenstein, D., Keith, D., Feinberg, A., Peter, T., & Stenke, A. (2019). Exploring accumulation-mode h2so4 versus so2 stratospheric sulfate geoengineering in a sectional aerosol-chemistry-climate model. *Atmospheric Chemistry and Physics*, *19*(7), 4877–4897. Retrieved from https://www.atmos-chem-phys.net/19/4877/2019/ doi: 10.5194/acp-19-4877-2019

Visioni, D., Pitari, G., Aquila, V., Tilmes, S., Cionni, I., Di Genova, G., & Mancini, E. (2017). Sulfate geoengineering impact on methane transport and lifetime: results from the geoengineering model intercomparison project (geomip). *Atmospheric Chemistry and Physics*, *17*(18), 11209–11226. Retrieved from https://www.atmos-chem-phys.net/17/11209/2017/ doi: 10.5194/acp-17-11209-2017

Visioni, D., Pitari, G., Tuccella, P., & Curci, G. (2018). Sulfur deposition changes under sulfate geoengineering conditions: Quasi-biennial oscillation effects on the transport and lifetime of stratospheric aerosols. *Atmospheric Chemistry and Physics*. doi: 10.5194/acp-18-2787-2018

Visioni, D., Slessarev, E., MacMartin, D., Mahowald, N. M., Goodale, C. L., & Xia, L. (2020). What goes up must come down: impacts of deposition in a sulfate geoengineering scenario. *Environmental Research Letters*. Retrieved from http://iopscience.iop.org/10.1088/1748-9326/ab94eb

Waugh, D. W., Sobel, A. H., & Polvani, L. M. (2017). What is the polar vortex and how does it influence weather? *Bulletin of the American Meteorological Society*, *98*(1), 37–44. doi: 10.1175/BAMS-D-15-00212.1

Wu, Y., Simpson, I. R., & Seager, R. (2019). Intermodel spread in the northern hemisphere stratospheric polar vortex response to climate change in the cmip5 models. *Geophysical Research Letters*, *46*(22), 13290-13298. Retrieved from `https://agupubs.onlinelibrary.wiley.com/doi/abs/10.1029/2019GL085545` doi: 10.1029/2019GL085545

Figure 1.

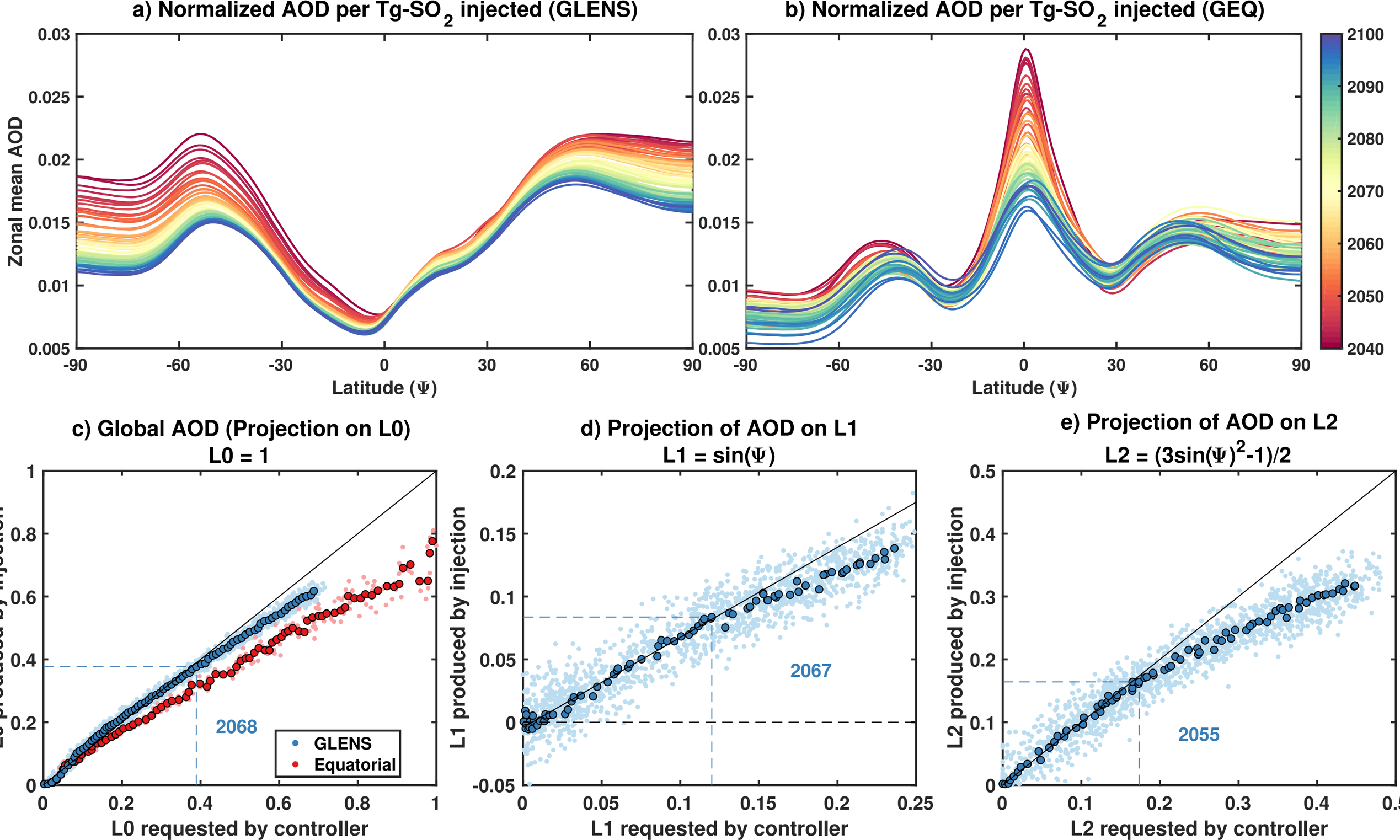
a) Normalized AOD per Tg-SO2 injected (GLENS)
b) Normalized AOD per Tg-SO2 injected (GEQ)
Zonal mean AOD
Latitude (Ψ)
2100
2090
2080
2070
2060
2050
2040
c) Global AOD (Projection on L0)
L0 = 1
L0 produced by injection
L0 requested by controller
2068
GLENS
Equatorial
d) Projection of AOD on L1
L1 = sin(Ψ)
L1 produced by injection
L1 requested by controller
2067
e) Projection of AOD on L2
L2 = (3sin(Ψ)2-1)/2
L2 produced by injection
L2 requested by controller
2055

Figure 2.

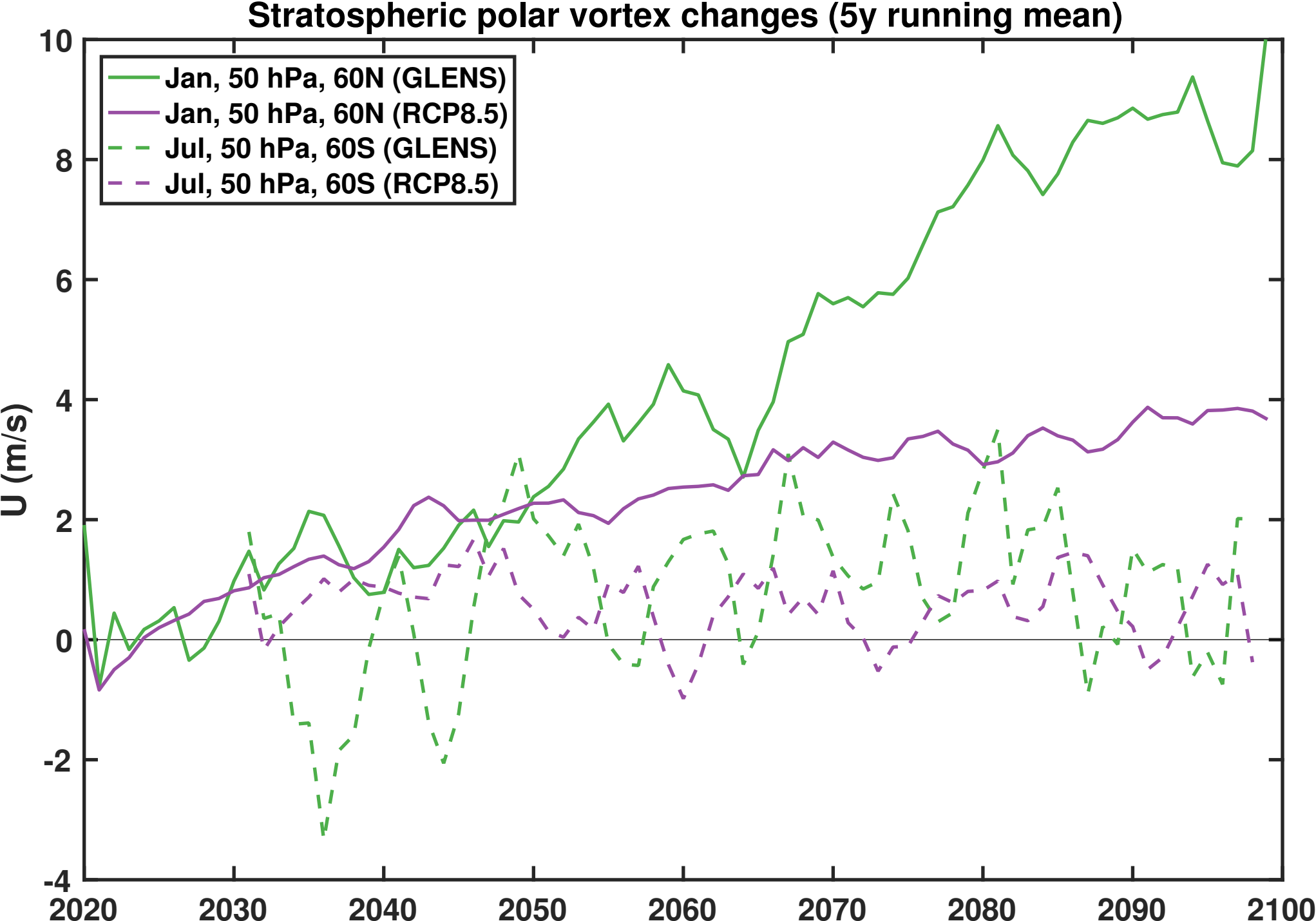
Stratospheric polar vortex changes (5y running mean)
Jan, 50 hPa, 60N (GLENS)
Jan, 50 hPa, 60N (RCP8.5)
Jul, 50 hPa, 60S (GLENS)
Jul, 50 hPa, 60S (RCP8.5)
U (m/s)
10
8
6
4
2
0
-2
-4
2020
2030
2040
2050
2060
2070
2080
2090
2100

Figure 3.

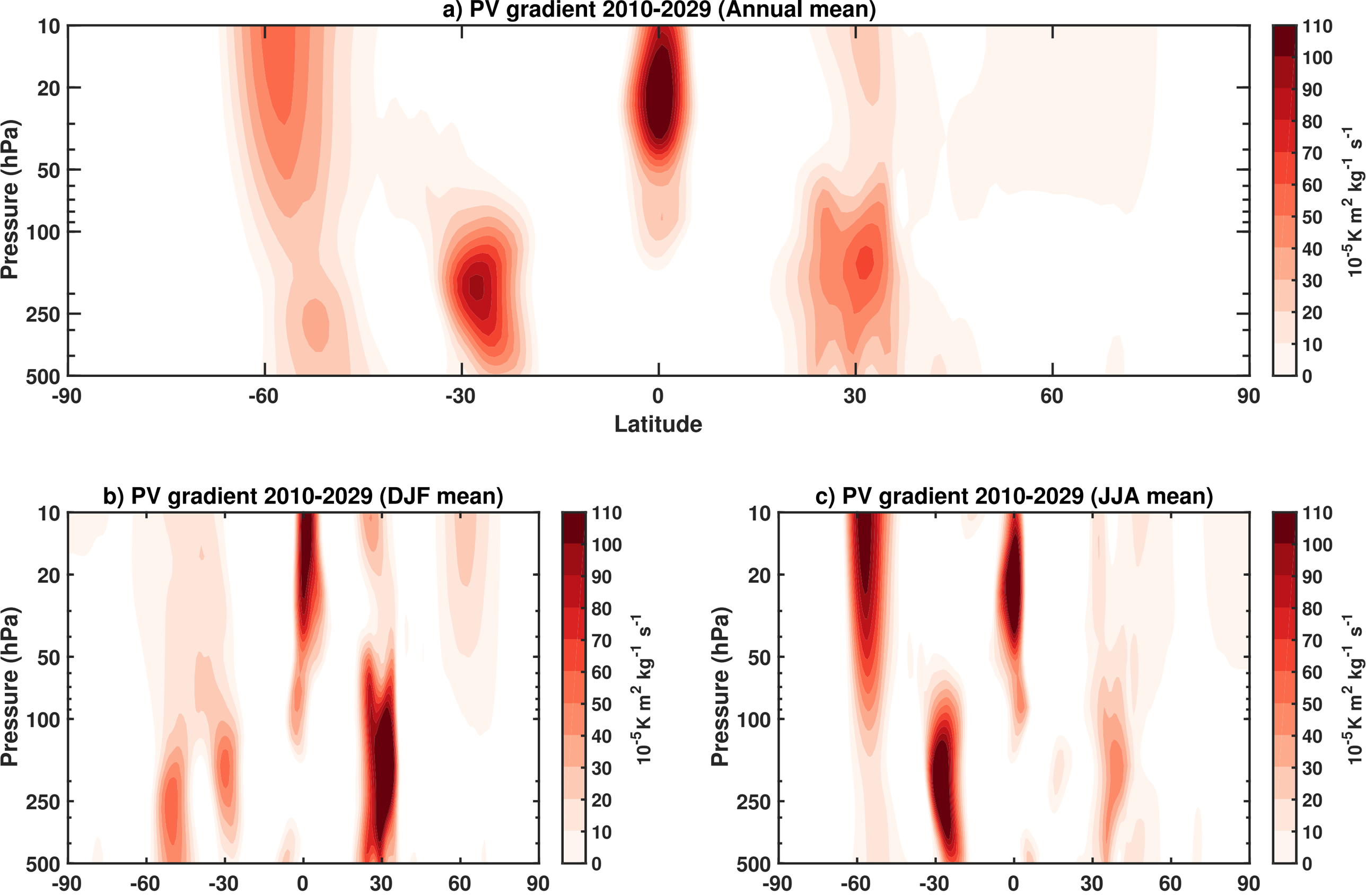
a) PV gradient 2010-2029 (Annual mean)
b) PV gradient 2010-2029 (DJF mean)
c) PV gradient 2010-2029 (JJA mean)
Pressure (hPa)
10
20
50
100
250
500
Latitude
-90
-60
-30
0
30
60
90
10^{-5}K m^2 kg^{-1} s^{-1}
110
100
90
80
70
60
50
40
30
20
10
0

Figure 4.

a) GLENS anomaly of PV latitudinal gradient at 50 hPa in DJF

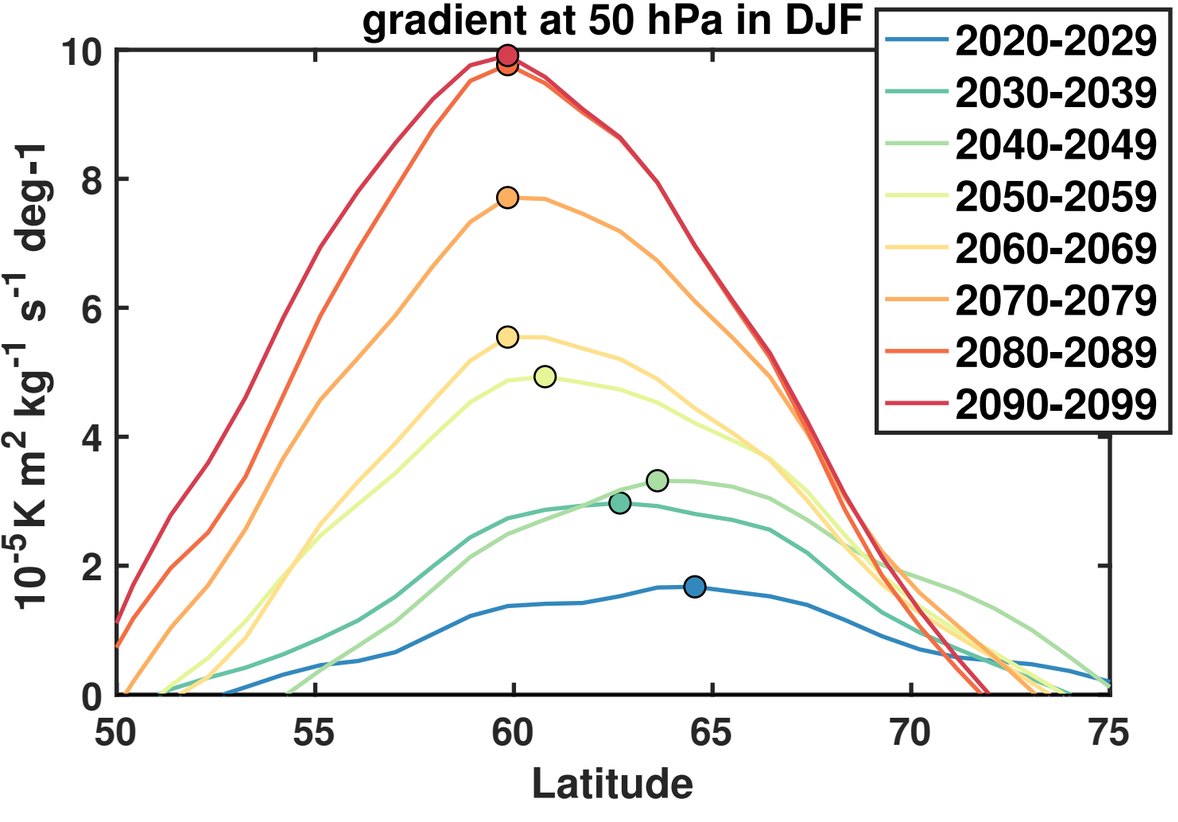

b) GLENS anomaly of PV latitudinal gradient at 50 hPa in JJA

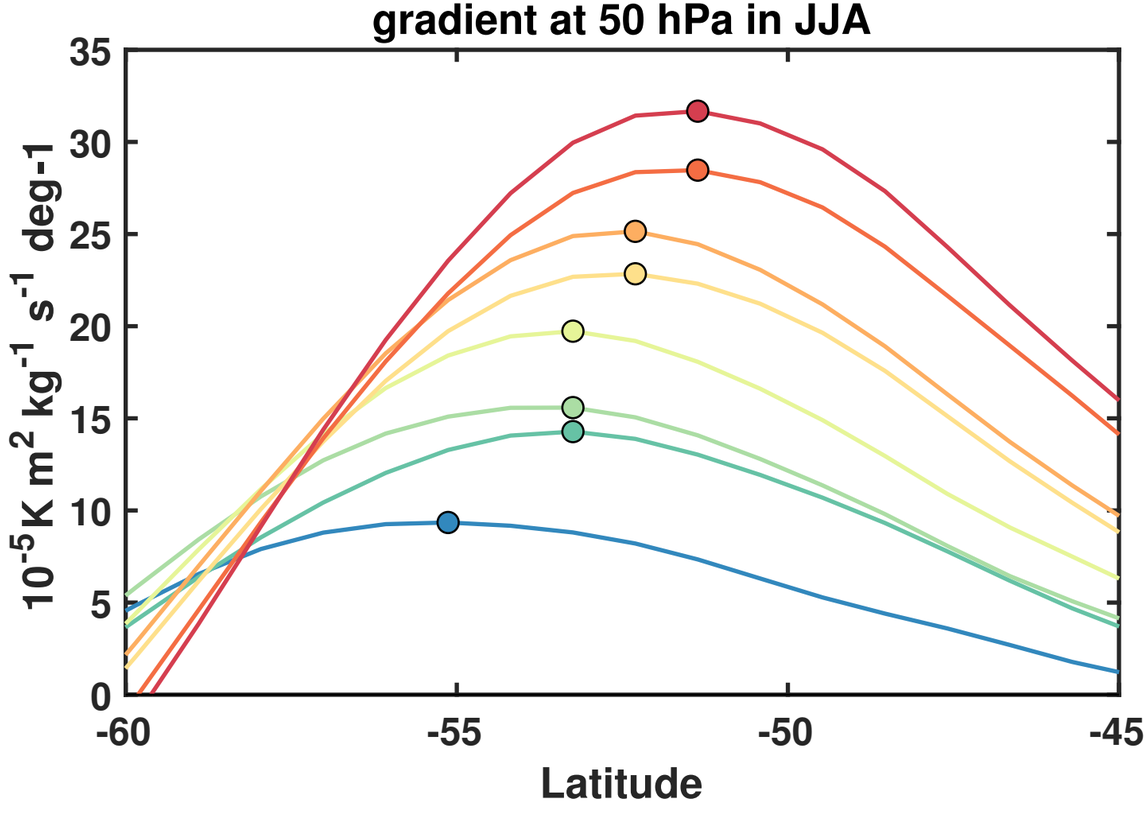

c) High latitudinal AOD efficiency